Journal of Molecular Liquids 246 (2017) 244–250

Contents lists available at ScienceDirect

Journal of Molecular Liquids

journal homepage: www.elsevier.com/locate/molliq

Effect of nanoparticles on vapour-liquid surface tension of water: A molecular dynamics study

Neha Sinha, Jayant K. Singh *

Department of Chemical Engineering, Indian Institute of Technology Kanpur, Kanpur, UP 208016, India

ARTICLE INFO

Article history:
Received 6 March 2017
Received in revised form 28 June 2017
Accepted 16 September 2017
Available online 19 September 2017

ABSTRACT

We study the effect of nanoparticles on the vapour-liquid surface tension of TIP4P/2005 water model using molecular dynamic simulations. The interactions of nanoparticles with water and volume percentage of nanoparticles are varied. It is found that the surface tension increases with increasing hydrophilicity and decreases with increasing hydrophobicity, as the nanoparticle volume percentage is increased. However, the surface tension values do not increase at higher volume fraction, both for hydrophilic and hydrophobic interactions. We also present the effect of temperature on the surface tension of water with nanoparticles. It is found that surface tension of water with hydrophobic nanoparticles reduces substantially faster with increasing temperature compared to that containing hydrophilic nanoparticles. The behaviour is well supported by the interfacial width data.

1. Introduction

Surface tension is the force experienced by molecules at any surface due to the difference in their nature on the two sides of it. It is called interfacial tension when the medium on both sides of the surface is other than air. Interfacial tension plays an important role in a number of industrial processes such as oil recovery [1,2], solid waste management [3]. It is useful in studying the amount of protein adsorbed at a fluid interface [4,5]. Interfacial tension values also determine how the organic wastes would dissipate in its environment [6]. The interfacial tension is one of the important factors in determining the movement of NAPL (non-aqueous phase liquids) within the subsurface at the sites of hazardous waste disposal [7].

Nanoparticles [8], due to their high surface to volume ratio, have brought evolution to the civilization as their "*all surface*" structure brings advancement to several applications, such as food and agriculture [9], drug delivery [10,11], paints [12] and emulsions [13], heat transfer [14], and several others. Many experimental studies have been conducted to see the effect of nanoparticles on interfacial tension. Depending upon the nature of the nanoparticles, the surface tension may get affected in their presence. Vafaei et al. [15] found that the surface tension of water in presence of bismuth telluride nanoparticles initially decreases with increase in volume percentage of nanoparticles (NPs), reaches a minimum and then increases. However, Tanvir and Qiao [16] found that the surface tension of water, ethanol and n-decane increases with increase in weight percentage of alumina NPs. Whereas Dong and Johnson [17] investigated the effect of charged stabilized TiO_2 NPs on surface tension of water and revealed that there is a decrease in surface tension with the increase in weight percentage of NPs, followed by an increase. Moreover, Okubo [18] observed that though surface tension of water remains unaffected in the presence of silica NPs, it is reduced by 20 mN/m in the presence of hydrophobic polystyrene (PS) NPs. Also, surface tension of water was found to be more susceptible to changes in the case of crystal like suspensions, such as PS NPs in water, than in the cases of liquid and gas like suspensions. In spite of the hydrophobicity of carbon nanotube, the surface tension of water with suspended CNTs was found to be higher than its intrinsic value as shown by Kumar and Milanova [19]. Glaser et al. [20] reported highest reduction in n-hexane/water interfacial tension with DDT capped Au-Fe_3O_4 Janus particles when compared to the reduction by Au and Fe_3O_4 NPs individually. Also, the interfacial tension was found to decrease with increase in the Janus NPs concentration.

Several authors have investigated the effect of nanoparticles on surface/interfacial tension of different systems using molecular simulations. Ranatunga et al. [21] carried out the molecular dynamics (MD) simulation of heptane-water interface and found that the uncharged NPs at oil-water interface do not alter the interfacial tension significantly. At low concentrations of surfactants, the NPs showed harmonious behaviour in reducing the oil-water interfacial tension, the effect being reduced at high surfactant concentrations. Fan et al. [22] simulated decane-water interface containing homogenous and Janus silica NPs functionalised with different percentage of methyl and hydroxyl groups to vary their hydrophobicity and hydrophilicity. However, no significant change in interfacial tension was reported. Luo et al. [23] too reported insignificant change in water/TCE (trichloroethylene) interfacial tension obtained from simulation of self-assembled modified hydrocarbon NPs at water-TCE interface. Lu et al. [24] performed MD simulations to

* Corresponding author.
E-mail address: jayantks@iitk.ac.in (J.K. Singh).

https://doi.org/10.1016/j.molliq.2017.09.059
0167-7322/

study the dynamic wetting of water nano-droplet with gold NPs on a gold substrate. They found that surface tension of water increased with increase in the nanoparticle (NP) loading.

Thus, these reports do not reflect any specific trend in the variation of surface/interfacial tension with the changes in NP concentrations around or at it. This reflects that surface/interfacial tension behaviour is specific to the systems involved in the study. MD is a powerful tool which can be used to study the system at molecular level [25], offering molecular insights which might not be possible through experiments. In this paper, we study the surface tension of water in the presence NPs of different affinities using MD simulations. In the next section, we present the model and methodology considered in this study. We will discuss the outcome of the work in the subsequent section followed by conclusions of this study.

2. Methods and models

We have used TIP4P/2005 water model [26] to prepare our model systems. The system consists of water with NPs. The structure of the NP is made by cutting a spherical particle from bulk FCC structure. Each NP is of 1 nm diameter, consisting of 43 atoms, arranged in FCC lattice with lattice constant of 4.080 Å. The NP is kept charge neutral and rigid during the simulations.

The non-bonded interactions between water molecules are described by the equation

$$U_{nonbond} = 4\varepsilon_{ij}\left[\left(\frac{\sigma_{ij}}{r_{ij}}\right)^{12} - \left(\frac{\sigma_{ij}}{r_{ij}}\right)^{6}\right] + \frac{q_i q_j}{4\pi\varepsilon_o r_{ij}} \quad (1)$$

where, ε_{ij} and σ_{ij} are the energy and length parameters of Lennard-Jones potential, respectively. The charges on the atoms i and j are represented by q_i, and q_j, respectively. r_{ij} denotes center to center distance and ε_o represents the dielectric permittivity constant. The non-bonded interaction between water-NP and NP-NP is represented using the Lennard–Jones potential function.

The hydrophilic NPs are modelled as gold NPs. The hydrophobic NPs are obtained from hydrophilic gold NPs by reducing the interaction strength between O of water and gold atom of NP by 4 times. The force field parameters for water, hydrophobic NPs and hydrophilic NPs are described in the Table 1.

All the simulations are run using LAMMPS package [27]. The equation of motion is integrated using velocity-Verlet algorithm with a time step of 0.001 ps. The simulations are carried out using NVT ensemble, where the number of particles, volume and temperature of the system are kept constant. Temperature is maintained at 300 K using Nosé-Hoover thermostat with a relaxation time of 0.1 ps. Surface tension values are collected over every 0.1 ps for analysis. The particle-particle particle-mesh (PPPM) technique [28] with kspace accuracy of 1.0e − 5 is used to compute the long range columbic interactions. The cutoff for both Lennard-Jones and electrostatic interactions of water and water-NP is 13 Å. Shake algorithm is used to keep the water molecules rigid. Periodic boundary condition is applied in all the three dimensions.

We have performed simulation for 4000 molecules of water. Initially, the box containing water molecules is simulated using the NPT ensemble to achieve equilibrium density. The box obtained at the end of NPT run is a cube with side length of ~48 Å. We have considered 8 volume percentages of nanoparticles viz., 1.72, 3.38, 4.98, 6.54, 7.67, 10.21, 12.27 and 14.87, in water to study the surface tension. The volume percentage is calculated as (volume of NP ∗ 100) / (volume of liquid water), where volume of liquid water is calculated at the end of NPT run.

In order to obtain vapour-liquid interface, the box length in the x direction is increased to three times of its original value. The simulation box becomes a cuboid (~144 × 48 × 48), with two vacuum–water (with or without nanoparticles) interfaces. The system is then subjected to NVT run for the estimation of surface tension.

The interfacial width is obtained by fitting the density profiles of water as obtained from our simulations to the following equation [29],

$$\rho(x) = \frac{1}{2}\left[(\rho_l + \rho_v) - (\rho_l - \rho_v)\ erf\left(\frac{\sqrt{\pi}(x - x_0)}{\sigma_e}\right)\right] \quad (2)$$

where ρ_l and ρ_v are density of water in liquid and vapour phase respectively. σ_e, x_0 are the interfacial width and position of Gibbs dividing surface respectively [30].

In molecular simulations, the total pressure is calculated as ensemble average of the instantaneous pressure [31]. In our simulations, the pressure is calculated using following equation [32],

$$P = \frac{Nk_BT}{V} + \frac{\sum_i^N r_i * f_i}{dV} \quad (3)$$

The first contribution to pressure is due to the kinetic energy of the molecules, where N is the number of the particles in the system, k_B is the Boltzmann constant, T is the absolute temperature and d is the dimensionality of the system. The second contribution is due to the static forces between particles, where r_i is position of ith particle and f_i is the force acting on it.

The macroscopic pressure is simply obtained by taking an ensemble average over instantaneous pressure. Thus the macroscopic pressure is given as

$$P = <\rho k_B T> + \left\langle \frac{1}{3V}\sum_i \sum_{j<1} r_{ij} f_{ij} \right\rangle, \quad (4)$$

where r_{ij} is the intermolecular distance vector between a molecular pair i and j; f_{ij} is the corresponding force vector.

System pressure at a point can be broken down into three components: P_{xx}, P_{yy} and P_{zz} which are the normal pressure components in the x, y and z directions respectively. In our case, P_{xx} is the normal component perpendicular to the vapour-liquid interface. P_{yy} and P_{zz} are the two tangential components where the total tangential pressure P_t is $\frac{1}{2}(P_{yy} + P_{zz})$. Mechanical equilibrium requires P_{xx} to be constant throughout the system [33,34].

The surface tension is computed using the approach developed by Tolman [35] and refined by Kirkwood and Buff [36], where it is computed as the difference between the normal and tangential components of pressure as in equation below,

$$\gamma = \int_{-\infty}^{\infty} \left(P^n(x) - P^t(x)dx\right) \quad (5)$$

where P^n and P^t are the normal and tangential components of pressure. The difference between the two components of pressure is integrated along the axis, normal to the vapour–liquid interface. The difference cancels out in the bulk where $P^n = P^t$. In MD simulations, the integral in Eq. (5) can be represented by the difference of the ensemble averages

Table 1
Interaction parameters for TIP4P/2005 water model and gold NPs.

Atom-atom	ε (kcal/mol)	σ (Å)
O-O [26]	0.1852	3.1589
O-Au (hydrophilic) [51]	0.59	3.6
O-Au (hydrophobic)	0.1475	3.6
H-Au	None	–
Au-Au [52]	0.039	2.935

as shown below [37],

$$\gamma = \frac{1}{2}\left[\langle P_{xx}\rangle - \frac{1}{2}\left(\langle P_{yy}\rangle + \langle P_{zz}\rangle\right)\right] \quad (6)$$

The factor $\frac{1}{2}$ accounts for the two vapour-liquid interfaces present in the system.

Each simulation is run for 5 ns and the data is collected every 0.1 ps. The surface tension calculated in our simulations is averaged over the last 3 ns. For the higher volume percentage viz., 12.27% and 14.87%, we have performed longer runs of 10 ns each to cover a large range of data for minimising the uncertainty in surface tension values. In this case, we have used last 8 ns data for the calculation of error bar.

In the current work, the reported surface tension values does not include tail corrections as our interest in this work is to examine the change in the behaviour of water surface tension using a suitable water model in presence of nanoparticles of different types.

3. Results and discussion

Fig. 1 shows the typical vapour-liquid density profile of water at 300 K with hydrophilic NPs. The plot in left panel shows the density profile of water with 1.72 vol% of NPs in it, where the NPs are seen to be within the liquid phase. The corresponding snapshot clearly shows their presence in the liquid phase. The density profile of NPs shows discrete peaks i.e., noise is rather large mainly due to lesser number of NPs present in the system. The local density of water is found to perturb with increase in volume percentage of NPs as seen for the case of 12.27% (see right panel of Fig. 1). The corresponding snapshot depicts strong preference of NPs to be within the bulk phase even at increased NP concentration. The stronger interactions between the water molecules and NPs essentially leads to localization of water molecules in the liquid phase and hence the fluctuation in liquid density. However, in the case of hydrophobic NPs, the density profiles, as shown in Fig. 2, clearly depict that the NPs prefer to stay at the interfaces. At a lower concentration of 1.72 vol%, most of the NPs stay at one interface, and so there is no symmetry in the density profile as seen in the left panel plot of Fig. 2. The corresponding snapshot clearly depicts that NPs prefer staying at the interface due to strong hydrophobicity. However, at a high concentration of 12.27 vol%, the number of NPs is large enough to occupy both the vapour-liquid interface leading to symmetry in their density profile as can be seen in the right panel plot of Fig. 2. This is clearly evident in the corresponding snapshot. As the number of NPs is more than the number, which can occupy the interfacial area, some of them move to the vapour region as can be seen in the snapshot. Moreover, there is no preferential forces for the NPs to stay close to each other, and thus due to small size and thermal fluctuations, they overcome the free-energy barrier and move into the vapour phase. This is primarily the reason for small peaks in the vapour region of the density profile.

In the density profiles, we observed that hydrophobic NPs preferred to stay at the interface (for 1.72 vol%) rather in either phase. At higher NP concentrations (12.27 vol%), the NPs showed similar preference with a few traversing the vapour phase. Thus, the NPs should have a strong effect on the interfacial width. To this end, we calculated the interfacial width using Eq. (2), the results are summarized in Table 2. Fig. 3 shows vapour-liquid interfacial width of water for both hydrophilic and hydrophobic NPs. With hydrophilic NPs, it is found that as the NP volume percentage increases, the interfacial width decreases as can be distinctly seen in Fig. 3. It can also be observed in the same figure that at increased NP concentrations, the interfacial width saturates and shows a plateau. On the other hand, with hydrophobic NPs, the interfacial width is found to increase with the increase in NP volume percentage, as seen in the figure. In this case too, we observe that at higher NP volume percent, the interfacial width ceases to change and reflects saturation in its values. For hydrophobic NPs, the interaction between them and water is of repulsive nature, so they have a tendency to recede from each other giving rise to perturbations at the interface. Accordingly, it can be concluded that the broadening of interfacial width in case of hydrophobic NPs is due to the disturbances caused by the NPs at the interface. For hydrophilic NPs in water, as the NP concentrations increase, they get in close proximity to the interface. Consequently, they exert an attractive pull at the interfacial water [38]. Due to these attractive forces, the interface become steeper, the width leaner and hence, a decrease in the interfacial width is observed. The broadening of interfacial width in the presence of NPs from hydrophilic to hydrophobic interactions can also be seen in Fig. 4.

Thus, from the interfacial data, we observed that the interfacial width is affected in the presence of NPs for both hydrophilic and hydrophobic interactions. It is well known from various theories that surface

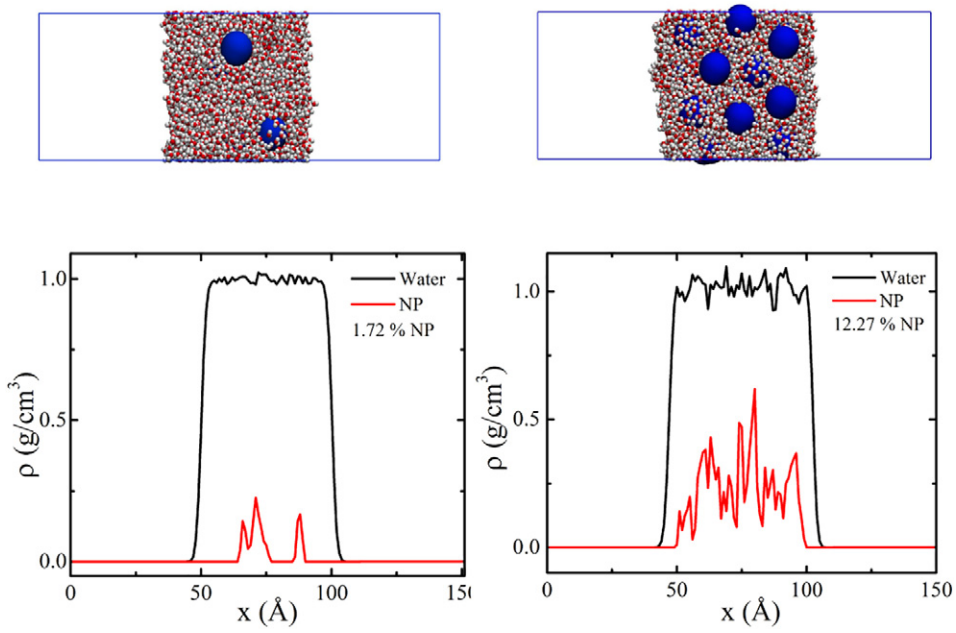

Fig. 1. Density profiles and the corresponding snapshots for NPs with hydrophilic interactions in 4000 molecules of water at 300 K. The interaction strength between water and NPs is $\varepsilon_{NP\text{-}W}$ = 0.59 kcal/mol. The profiles correspond to 1.72 and 12.27 vol% of NPs in water.

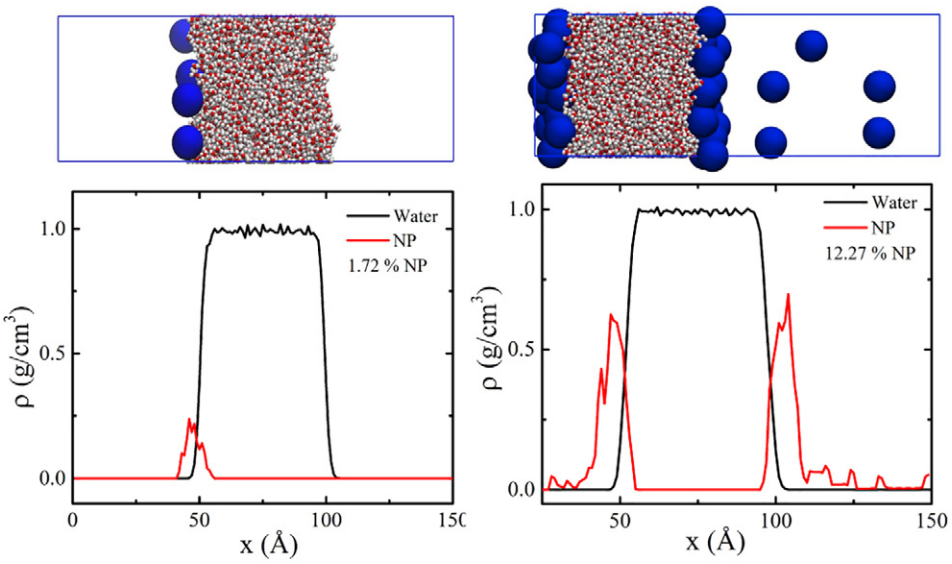

Fig. 2. Density profiles and the corresponding snapshots for NPs with hydrophobic interactions in 4000 molecules of water at 300 K. The interaction strength between water and NPs is $\varepsilon_{NP\text{-}W} = 0.1475$ kcal/mol. The profiles correspond to 1.72 and 12.27 vol% of NPs in water.

tension is strongly dependent on the interfacial width [39]. Thus, the surface tension of water, should get affected in the presence of such NPs. To see the effect, we calculated the surface tension of water-NP system as the integral of the difference of normal and tangential pressure components given by Eq. (6), which adequately means that surface tension at any surface comes to play due to the difference between the normal and tangential components of pressure at it.

Fig. 5 shows the variation of surface tension of water at different volume percentage of NPs. It should be noted that the surface tension of the TIP4P/2005 water model without the long range corrections obtained in our simulations is in line with the result reported by Vega and de Miguel [40] and Pascal and Goddard [41]. Water with hydrophilic NPs does not show any specific trend in surface tension values up to 6.54 NP vol%. However, as the volume percentage increases, the surface tension value increases noticeably. At high NP concentration, the NPs exert large effective attractive pull at the interfacial water molecules. This leads to stiffer interface which is quantified in terms of increased value of surface tension. The increase in surface tension of water with these hydrophilic NPs is also well supported by the interfacial width data (see Figs. 3 and 4) which show a decrease in average values of interfacial width with the increase in NP concentration. Several experiments have been carried out to study the effect of NP concentration variation on the surface/interfacial tension of different systems. Our results reinforce the experimental observations which suggest an increase in surface/interfacial tension of systems with increase in NP concentration for the hydrophilic NP-water interactions [16,42–44].

In Fig. 5, water with hydrophobic NPs shows a decrease in the average value of surface tension with increasing NP concentration within the system. The accumulation of NPs at the interface results in weaker interaction between surface water molecules which causes reduction in surface tension. The decrease in surface tension is well reinforced by interfacial data which shows an increase in average values of interfacial width with increase in NP concentration. However, at high concentration, the changes in surface tension are not much and are observed to be mostly overlapping. Our result is in line with the experimental observation, which suggests that surface tension decreases with increase in hydrophobic extent of the system [45].

It was proposed by Stillinger more than three decades ago that hydrogen bonding of water disrupts in the vicinity of large hydrophobic solutes (solute radius > 1 nm) [46]. The NP radius considered in our simulation is of 0.5 nm but the volume percentage is varied from 1.72 (4 NPs) to 14.87 (40 NPs) percentage. In order to ascertain if the hydrogen bonding between the water molecules at the surface get affected in our system of water with NPs of size 1 nm, we perform a hydrogen bonding analysis for the case of hydrophobic NPs, using the binning procedure, similar to that used in calculating the density profiles of water. We have considered two water molecules hydrogen bonded if the following three conditions are satisfied [47], $R_{OO} < 3.5$ Å, $R_{OH} < 2.60$ Å and HO···O angle $< 30^{\circ}$. Fig. 6 shows the hydrogen bond values at the interfacial region of water and water with three different NP volume percentage (1.72, 7.67 and 12.27). It can be seen that the graphs have overlapping values for average hydrogen bonds per molecule. Thus, the hydrogen bonds at the interface are not affected significantly in the presence of NPs (of size 1 nm) at different volume percentage.

In order to see the effect of temperature on the surface tension behaviour of water in presence of NPs, we conducted simulation at various

Table 2
Interfacial width and surface tension values for water-hydrophilic NPs ($\varepsilon_{NP\text{-}W} = 0.59$ kcal/mol) and water-hydrophobic NPs ($\varepsilon_{NP\text{-}W} = 0.1475$ kcal/mol), for eight different volume percentage of NPs in water. All the values are reported at 300 K.

NP vol%	Surface tension (mN/m) (hydrophilic interactions)	Interfacial width (Å)	Surface tension (mN/m) (hydrophobic interactions)	Interfacial width (Å)
0	63.51 (69)	3.63 (4)		
1.72	64.02 (86)	3.57 (006)	63.03 (39)	3.86 (006)
3.98	64.14 (224)	3.58 (2)	62.82 (185)	4.01 (14)
4.98	65.99 (145)	3.50 (004)	61.26 (163)	4.38 (11)
6.53	66.00 (314)	3.36 (005)	61.36 (229)	4.52 (16)
7.67	68.28 (352)	3.26 (009)	61.31 (192)	4.72 (009)
10.21	70.82 (175)	2.94 (13)	57.99 (158)	4.75 (11)
12.27	77.96 (391)	3.08 (17)	55.06 (303)	4.68 (007)
14.87	79.84 (353)	3.06 (17)	48.77 (241)	4.69 (17)

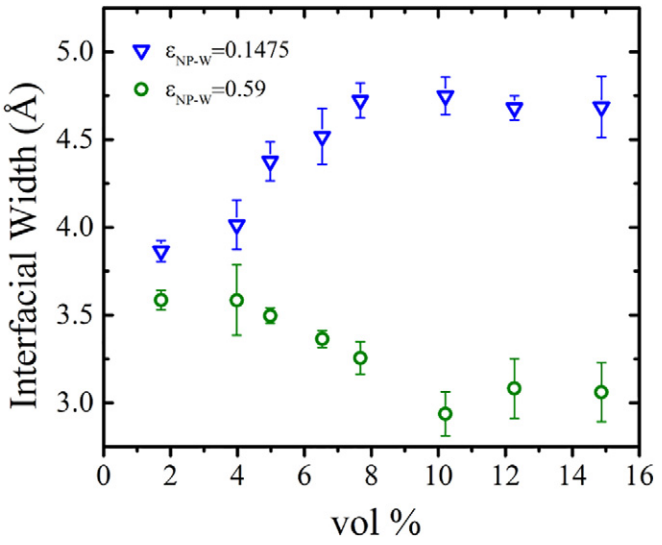

Fig. 3. Interfacial width of water with NPs of hydrophobic and hydrophilic interactions, as a function of NP volume percentage at 300 K. ε_{NP-W} inset shows the value of interaction strength between water and NPs in kcal/mol.

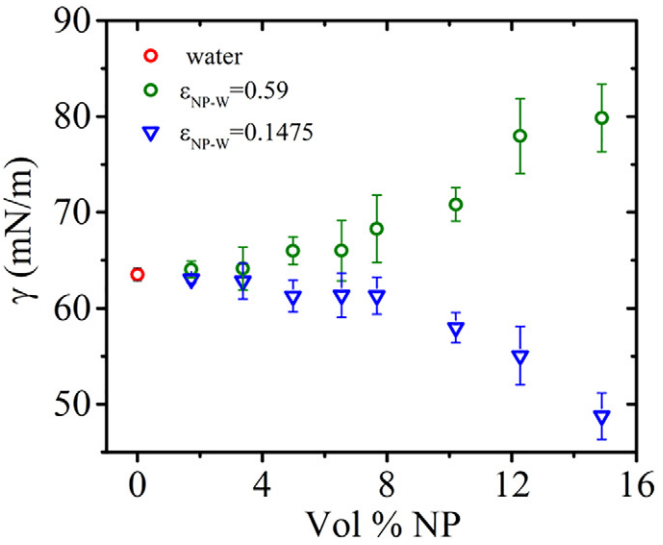

Fig. 5. Surface tension of water with NPs of hydrophobic and hydrophilic interactions, as a function of volume percentage of NP at 300 K. ε_{NP-W} inset shows the value of interaction strength between water and NPs in kcal/mol.

temperatures. Figs. 7 and 8 show the surface tension of TIP4P/2005 model of water in the temperature range of 300 K to 425 K in the presence hydrophilic and hydrophobic NPs, respectively. Though the NPs affect the interfacial tension as discussed above depending on their nature, the temperature response of surface tension remain the same i.e., surface tension decreases with increase in temperature. This is also in line with several experimental works [45,48–50] which have shown that the interfacial/surface tension of oil/water and water base fluids decreases with increase in temperature. Nevertheless, there is an inherent difference in the way hydrophilic NPs embedded water respond to temperature as compared to the case of hydrophobic NPs. Hydrophilic NPs system have larger cohesive energy due to which the temperature required to change the surface tension by unit value is much larger than the case of hydrophobic NPs. This is more evident at higher volume percentage. For example, at 12.27 NP vol%, the change in the surface tension value with respect to the pure case is 23% to 43% with increase in the temperature from 300 K to 425 K. In other words, the hydrophilic NPs make it difficult for water molecules to move from the liquid phase to the vapour phase, leading to relatively much higher surface tension at higher temperature with respect to the pure case. On the contrary, this phenomenon is missing in hydrophobic NPs + water system, where hydrophobic NPs promote water molecules to the vapour phase by displacing it from the interface. This behaviour is enhanced with increasing number of NPs as suggested by the drop in the surface tension value with increasing volume percentage of NPs. However, this behaviour is not affected by the temperature, and the change in the surface tension value with respect to the pure case is more or less constant; for example it is around ~1.5% and ~12% for 4.98% and 12.27% NPs, respectively.

4. Conclusion

The surface tension of TIP4P/2005 water in the presence of NPs of hydrophilic and hydrophobic interactions is investigated using molecular dynamics simulations. The average value of surface tension is found to increase with increasing number of NPs for the case of hydrophilic interactions. However, contrary behaviour is observed for hydrophobic

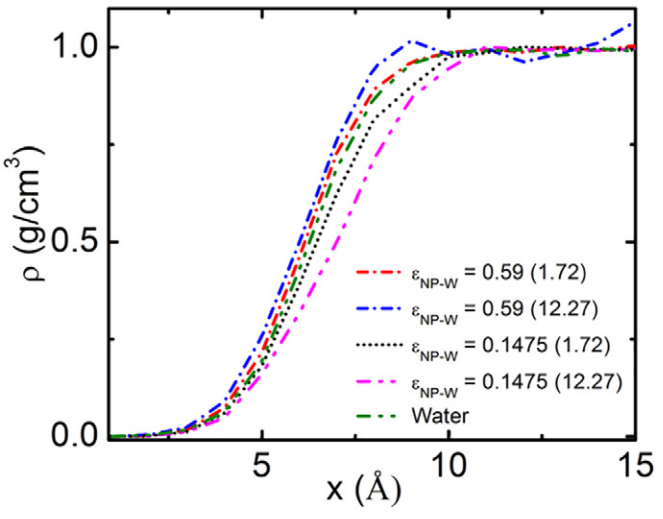

Fig. 4. Interfacial width of water with different volume percentage of NPs (1.72 and 12.27 vol%) at 300 K. ε_{NP-W} inset shows the value of interaction strength between water and NPs in kcal/mol.

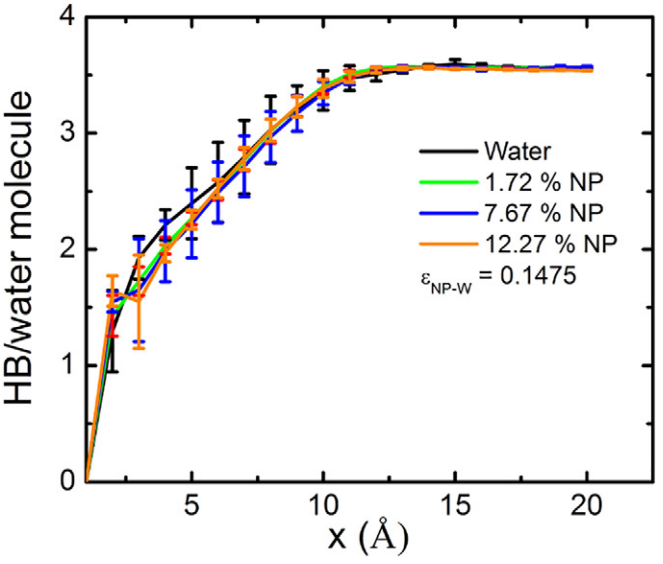

Fig. 6. Hydrogen bonding for water with different volume percentage of NPs at 300 K. ε_{NP-W} inset shows the value of interaction strength between water and NPs in kcal/mol.

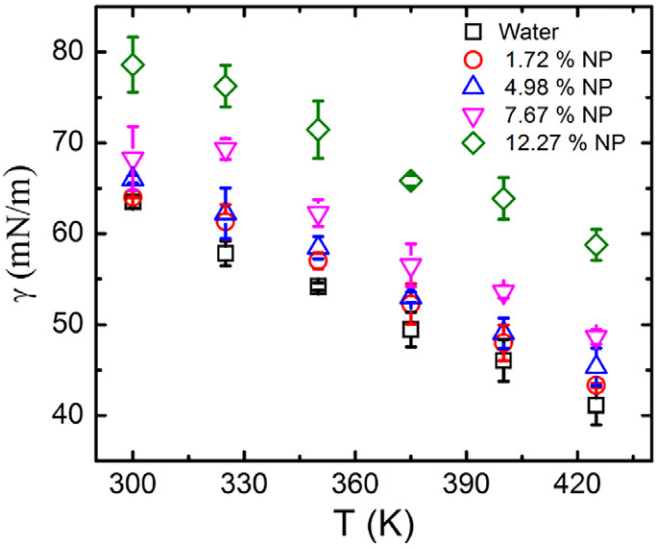

Fig. 7. Surface tension of water with different volume percentage (shown inset) of hydrophilic NPs. The interaction strength between water and NPs is $\varepsilon_{NP\text{-}W} = 0.59$ kcal/mol.

NPs. Such a trend is well supported by the corresponding interfacial width data, the average value of which is found to decrease in the presence of hydrophilic NPs. This decrease in value is attributed to the attractive pull exerted by the NPs in bulk over the surface water molecules. For hydrophobic NPs, the average interfacial width is found to increase with NPs volume percentage. For both hydrophilic and hydrophobic NPs, the interfacial is found to saturate at increased volume percentage. This is also reflected in the surface tension values which do not change significantly at higher concentration. The NPs of size 1 nm at the vapour-liquid interface, for the case of hydrophobic interactions do not disturb the hydrogen bonding structure for different volume percentage considered. The effect of temperature on the vapour-liquid surface tension of water containing NPs is also studied. It was found that hydrophilic NPs reduce the response of temperature on the surface tension.

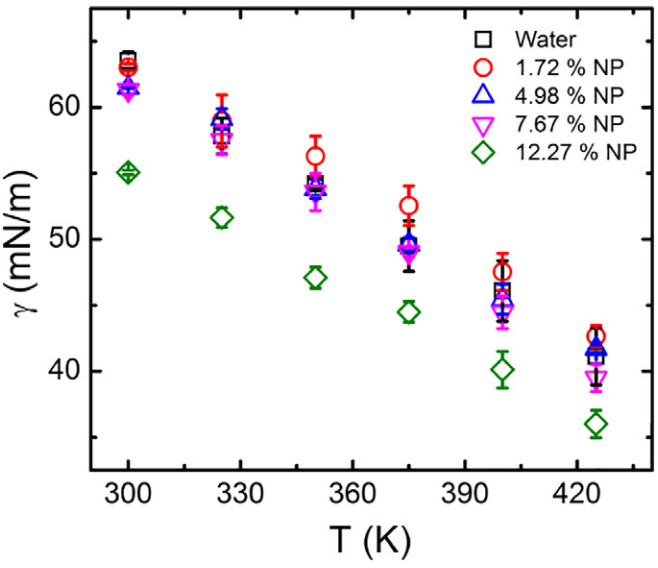

Fig. 8. Surface tension of water with different volume percentage (shown inset) of hydrophobic NPs. The interaction strength between water and NPs is $\varepsilon_{NP\text{-}W} = 0.1475$ kcal/mol.

Acknowledgements

This work is supported by the Council of Scientific and Industrial Research (CSIR) (22(0675)/14/EMR-II) and Department of Science and Technology, Government of India (SB/S3/CE/079/2015).

References

[1] Y. Touhami, D. Rana, V. Hornof, G.H. Neale, Effects of added surfactant on the dynamic interfacial tension behavior of acidic oil/alkaline systems, J. Colloid Interface Sci. 239 (2001) 226–229.
[2] M.J. Rosen, H. Wang, P. Shen, Y. Zhu, Ultralow interfacial tension for enhanced oil recovery at very low surfactant concentrations, Langmuir 21 (2005) 3749–3756.
[3] A. Bagchi, Design of Landfills and Integrated Solid Waste Management, John Wiley & Sons. Inc., 2004
[4] C.J. Beverung, C.J. Radke, H.W. Blanch, Protein adsorption at the oil/water interface: characterization of adsorption kinetics by dynamic interfacial tension measurements, Biophys. Chem. 81 (1999) 59–80.
[5] B.C. Tripp, J.J. Magda, J.D. Andrade, Adsorption of globular proteins at the air/water Interface as measured via dynamic surface tension: concentration dependence, mass-transfer considerations, and adsorption kinetics, J. Colloid Interface Sci. 173 (1995) 16–27.
[6] A.H. Demond, A.S. Lindner, Estimation of interfacial tension between organic liquids and water, Environ. Sci. Technol. 27 (1993) 2318–2331.
[7] J.W. Mercer, R.M. Cohen, A review of immiscible fluids in the subsurface: properties, models, characterization and remediation, J. Contam. Hydrol. 6 (1990) 107–163.
[8] J. Kreuter, Nanoparticles—a historical perspective, Int. J. Pharm. 331 (2007) 1–10.
[9] P. Sanguansri, M.A. Augustin, Nanoscale materials development – a food industry perspective, Trends Food Sci. Technol. 17 (2006) 547–556.
[10] X.C. Yang, B. Samanta, S.S. Agasti, Y. Jeong, Z.J. Zhu, S. Rana, O.R. Miranda, V.M. Rotello, Drug delivery using nanoparticle-stabilized nanocapsules, Angew. Chem. Int. Ed. Eng. 50 (2011) 477–481.
[11] W.H. De Jong, P.J.A. Borm, Drug delivery and nanoparticles: applications and hazards, Int. J. Nanomedicine 3 (2008) 133–149.
[12] A. Kumar, P.K. Vemula, P.M. Ajayan, G. John, Silver-nanoparticle-embedded antimicrobial paints based on vegetable oil, Nat. Mater. 7 (2008) 236–241.
[13] T.N. Hunter, R.J. Pugh, G.V. Franks, G.J. Jameson, The role of particles in stabilising foams and emulsions, Adv. Colloid Interf. Sci. 137 (2008) 57–81.
[14] S.M. You, J.H. Kim, K.H. Kim, Effect of nanoparticles on critical heat flux of water in pool boiling heat transfer, Appl. Phys. Lett. 83 (2003) 3374.
[15] V. Saeid, P. Arup, J. Abhishek, R. Ganapathiraman, B.-T. Theodorian, The effect of nanoparticles on the liquid–gas surface tension of Bi_2Te_3 nanofluids, Nanotechnology 20 (2009) 185702.
[16] S. Tanvir, L. Qiao, Surface tension of nanofluid-type fuels containing suspended nanomaterials, Nanoscale Res. Lett. 7 (2012) 1–10.
[17] L. Dong, D. Johnson, Interfacial tension measurements of colloidal suspensions: an explanation of colloidal particle-driven interfacial flows, Adv. Space Res. 32 (2003) 149–153.
[18] T. Okubo, Surface tension of structured colloidal suspensions of polystyrene and silica spheres at the air-water interface, J. Colloid Interface Sci. 171 (1995) 55–62.
[19] R. Kumar, D. Milanova, Effect of surface tension on nanotube nanofluids, Appl. Phys. Lett. 94 (2009), 073107.
[20] N. Glaser, D.J. Adams, A. Böker, G. Krausch, Janus particles at liquid–liquid interfaces, Langmuir 22 (2006) 5227–5229.
[21] R.J.K.U. Ranatunga, C.T. Nguyen, B.A. Wilson, W. Shinoda, S.O. Nielsen, Molecular dynamics study of nanoparticles and non-ionic surfactant at an oil–water interface, Soft Matter 7 (2011) 6942.
[22] H. Fan, D.E. Resasco, A. Striolo, Amphiphilic silica nanoparticles at the decane-water interface: insights from atomistic simulations, Langmuir 27 (2011) 5264–5274.
[23] M. Luo, O.A. Mazyar, Q. Zhu, M.W. Vaughn, W.L. Hase, L.L. Dai, Molecular dynamics simulation of nanoparticle self-assembly at a liquid–liquid interface, Langmuir 22 (2006) 6385–6390.
[24] G. Lu, H. Hu, Y. Duan, Y. Sun, Wetting kinetics of water nano-droplet containing nonsurfactant nanoparticles: a molecular dynamics study, Appl. Phys. Lett. 103 (2013) 253104.
[25] R. Petrenko, J. Meller, Molecular Dynamics, eLS, John Wiley & Sons, Ltd, 2001.
[26] J.L. Abascal, C. Vega, A general purpose model for the condensed phases of water: TIP4P/2005, J. Chem. Phys. 123 (2005) 234505.
[27] S. Plimpton, Fast parallel algorithms for short range molecular dynamics, J. Comput. Phys. 117 (1995) 1–19.
[28] A.Y. Toukmaji, J.A. Board Jr., Ewald summation techniques in perspective: a survey, Comput. Phys. Commun. 95 (1996) 73–92.
[29] J.D. Weeks, Structure and thermodynamics of the liquid–vapor interface, J. Chem. Phys. 67 (1977) 3106–3121.
[30] H.J. Butt, K. Graf, M. Kappl, Physics and Chemistry of Interfaces, John Wiley & Sons, Germany, 2006.
[31] M.P. Allen, D.J. Tildesley, Computer Simulation of Liquids, Clarendon, Oxford, 1987.
[32] A.P. Thompson, S.J. Plimpton, W. Mattson, General formulation of pressure and stress tensor for arbitrary many-body interaction potentials under periodic boundary conditions, J. Chem. Phys. 131 (2009) 154107.
[33] F. Varnik, J. Baschnagel, K. Binder, Molecular dynamics results on the pressure tensor of polymer films, J. Chem. Phys. 113 (2000) 4444–4453.
[34] M.V. Berry, The molecular mechanism of surface tension, Phys. Educ. 6 (1971) 79.

[35] R.C. Tolman, Consideration of the Gibbs theory of surface tension, J. Chem. Phys. 16 (1948) 758.
[36] J.G. Kirkwood, F.P. Buff, The statistical mechanical theory of surface tension, J. Chem. Phys. 17 (1949) 338.
[37] J. Alejandre, G.A. Chapela, The surface tension of TIP4P/2005 water model using the Ewald sums for the dispersion interactions, J. Chem. Phys. 132 (2010), 014701.
[38] J. Mittal, G. Hummer, Static and dynamic correlations in water at hydrophobic interfaces, Proc. Natl. Acad. Sci. U. S. A. 105 (2008) 20130–20135.
[39] T.B. Peery, G.T. Evans, Interface profiles in a dimerizing system, J. Chem. Phys. 114 (2001) 2387.
[40] C. Vega, E. de Miguel, Surface tension of the most popular models of water by using the test-area simulation method, J. Chem. Phys. 126 (2007) 154707.
[41] T.A. Pascal, W.A. Goddard, Interfacial thermodynamics of water and six other liquid solvents, J. Phys. Chem. B 118 (2014) 5943–5956.
[42] A.K.M.S. Islam, M.R. Amin, M. Ali, T. Setoguchi, M.H.U. Bhuiyan, R. Saidur, M.A. Amalina, R.M. Mostafizur, A. Islam, The 6th BSME international conference on thermal engineering effect of nanoparticles concentration and their sizes on surface tension of nanofluids, Procedia Eng. 105 (2015) 431–437.
[43] S.J. Kim, I.C. Bang, J. Buongiorno, L.W. Hu, Surface wettability change during pool boiling of nanofluids and its effect on critical heat flux, Int. J. Heat Mass Transf. 50 (2007) 4105–4116.
[44] M. Moosavi, E.K. Goharshadi, A. Youssefi, Fabrication, characterization, and measurement of some physicochemical properties of ZnO nanofluids, Int. J. Heat Fluid Flow 31 (2010) 599–605.
[45] J. Saien, F. Moghaddamnia, H. Bamdadi, Interfacial tension of methylbenzene–water in the presence of hydrophilic and hydrophobic alumina nanoparticles at different temperatures, J. Chem. Eng. Data 58 (2013) 436–440.
[46] F.H. Stillinger, Structure in aqueous solutions of nonpolar solutes from the standpoint of scaled-particle theory, J. Solut. Chem. 2 (1973) 141–158.
[47] A. Luzar, D. Chandler, Hydrogen-bond kinetics in liquid water, Nature 379 (1996) 55–57.
[48] J. Chinnam, D.K. Das, R.S. Vajjha, J.R. Satti, Measurements of the surface tension of nanofluids and development of a new correlation, Int. J. Therm. Sci. 98 (2015) 68–80.
[49] J. Saien, A. Rezvani Pour, S. Asadabadi, Interfacial tension of the n-hexane–water system under the influence of magnetite nanoparticles and sodium dodecyl sulfate assembly at different temperatures, J. Chem. Eng. Data 59 (2014) 1835–1842.
[50] S.M.S. Murshed, T. Say-Hwa, N. Nam-Trung, Temperature dependence of interfacial properties and viscosity of nanofluids for droplet-based microfluidics, J. Phys. D. Appl. Phys. 41 (2008), 085502.
[51] S. Merabia, Heat transfer from nanoparticles: a corresponding state analysis, Proc. Natl. Acad. Sci. U. S. A. 106 (2009) 15113–15118.
[52] P.K. Ghorai, Molecular dynamics simulation study of self assembled monolayers of alkanethiol surfactants on spherical gold nanoparticles, J. Phys. Chem. C 111 (2007) 15857–15862.